Dipyridyl β-diketonate complexes and their use as metalloligands in the formation of mixed-metal coordination networks

Andrew D. Burrows,*[a] Mary F. Mahon,*[a] Catherine L. Renouf,[a] Christopher Richardson,[a,b] Anna J. Warren[a] and John E. Warren[c]

[a] Department of Chemistry, University of Bath, Claverton Down, Bath BA2 7AY, UK. Fax: 44 1225 386231; Tel: 44 1225 386529; E-mail: a.d.burrows@bath.ac.uk, m.f.mahon@bath.ac.uk.

[b] School of Chemistry, University of Wollongong, Wollongong, NSW 2522, Australia.

[c] CLRC Daresbury Laboratory, Daresbury, Warrington WA4 4AD, UK.

Abstract

The iron(III) and aluminium(III) complexes of 1,3-di(4-pyridyl)propane-1,3-dionato (dppd) and 1,3-di(3-pyridyl)propane-1,3-dionato (dmppd), [Fe(dppd)$_3$] **1**, [Fe(dmppd)$_3$] **2**, [Al(dppd)$_3$] **3** and [Al(dmppd)$_3$] **4** have been prepared. These complexes adopt molecular structures in which the metal centres contain distorted octahedral geometries. In contrast, the copper(II) and zinc(II) complexes [Cu(dppd)$_2$] **5** and [Zn(dmppd)$_2$] **6** both form polymeric structures in which coordination of the pyridyl groups into the axial positions of neighbouring metal centres links discrete square-planar complexes into two-dimensional networks. The europium complex [Eu(dmppd)$_2$(H$_2$O)$_4$]Cl·2EtOH·0.5H$_2$O **7** forms a structure containing discrete cations that are linked into sheets through hydrogen bonds, whereas the lanthanum complex [La(dmppd)$_3$(H$_2$O)]·2H$_2$O **8** adopts a one-dimensional network structure, connected into sheets by hydrogen bonds. The iron complexes **1** and **2** act as metalloligands in reactions

with silver(I) salts, with the nature of the product depending on the counter-ions present. Thus, the reaction between **1** and $AgBF_4$ gave $[AgFe(dppd)_3]BF_4 \cdot DMSO$ **9**, in which the silver centres link the metalloligands into discrete nanotubes, whereas reactions with $AgPF_6$ and $AgSbF_6$ gave $[AgFe(dppd)_3]PF_6 \cdot 3.28DMSO$ **10** and $[AgFe(dppd)_3]SbF_6 \cdot 1.25DMSO$ **11**, in which the metalloligands are linked into sheets. In all three cases, only four of the six pyridyl groups present on the metalloligands are coordinated. The reaction between **2** and $AgNO_3$ gave $[Ag_2Fe(dmppd)_3(ONO_2)]NO_3 \cdot MeCN \cdot CH_2Cl_2$ **12**. Compound **12** adopts a layer structure in which all pyridyl groups are coordinated to silver centres and, in addition, a nitrate ion bridges between two silver centres. A similar structure is adopted by $[Ag_2Fe(dmppd)_3(O_2CCF_3)]CF_3CO_2 \cdot 2MeCN \cdot 0.25CH_2Cl_2$ **13**, with a bridging trifluoroacetate ion playing the same role as the nitrate ion in **12**.

Introduction

Metal-organic frameworks (MOFs) are currently attracting considerable attention, largely as a consequence of their porosity and subsequent use for applications such as hydrogen storage, carbon capture, separations and catalysis.[1] Mixed metal-organic frameworks (MMOFs) are an interesting sub-class of these materials, and given that two types of metal ion may have different structural and/or functional roles within a network structure, these are likely to attract increasing attention in the future. While it is possible to prepare MMOFs in a one-pot reaction, it can be difficult to control the nature of the products in this way. This has led to the development of a stepwise synthetic approach towards these materials. In the first step, a metal centre is reacted with a bifunctional ligand to give an isolable intermediate complex. This complex, termed a metalloligand, can itself act as a ligand in a second step, coordinating

to a different metal centre leading to the targetted mixed-metal coordination network structure.[2]

A number of metalloligands have been previously utilised in this manner, including complexes of pyridinedicarboxylates,[3] Schiff bases[4] and bis(oxamato) ligands,[5] that function as ditopic *O*-donors, and pyridyl-functionalised porphyrins,[6] dipyrrinato ligands,[7] terpyridines[8] and tris(triazolyl)borates,[9] that function as polytopic *N*-donors. Bifunctional ligands based on β-diketonates are attractive for use in construction of mixed-metal coordination networks, as the chelating nature of the bidentate *O,O*-donor ensures relatively low lability, and the negative charge on the ligand allows access to neutral complexes. We have previously prepared MMOFs based on 3-cyanoacetylacetonate metalloligands,[10] whereas Carlucci and co-workers have reported materials based on 1,3-di(4-cyanophenyl)propane-1,3-dionato metalloligands.[11] Pyridyl-functionalised β-diketonates have also attracted some attention. In particular, the Domasevitch[12] and Maverick[13] groups have prepared MMOFs based on 3-(4-pyridyl)acetylacetonate, whereas monometallic networks have also been prepared with pyridyl-substituted β-diketonates.[14, 15]

We recently communicated the use of the 1,3-di(4-pyridyl)propane-1,3-dionato ligand (dppd) to prepare the octahedral complexes [Al(dppd)$_3$] **3** and [Ga(dppd)$_3$].[16] These compounds are metalloligands containing six exotopic pyridyl groups, so have the potential to act as octahedral nodes. We demonstrated that reaction of these complexes with silver(I) nitrate gave [Ag$_3$M(dppd)$_3$](NO$_3$)$_3$·*x*DMSO (M = Al, Ga), in which the silver centres bridge between metalloligands leading to interpenetrated cubic networks.

In this paper we report the synthesis of dppd complexes containing iron, aluminium and copper. We also detail the use of the isomeric ligand 1,3-di(3-pyridyl)propane-1,3-dionato (dmppd) in the synthesis of iron, aluminium, zinc, europium and lanthanum compounds. Finally, we describe the reactions of the iron metalloligands $[Fe(dppd)_3]$ and $[Fe(dmppd)_3]$ with a range of silver(I) salts to form mixed-metal networks. While this paper was in preparation, reactions of $[Fe(dppd)_3]$ with silver(I) salts were reported by Carlucci and co-workers.[17] We compare and contrast our observations with theirs, showing the important effect of the solvent on the nature of the isolated product.

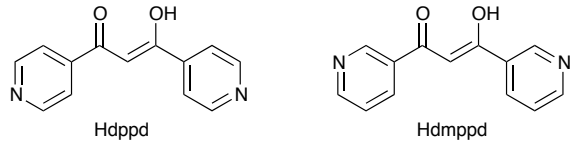

Hdppd Hdmppd

Results and Discussion

Synthesis of dppd and dmppd complexes

The complexes $[Fe(dppd)_3]$ **1** and $[Fe(dmppd)_3]$ **2** were prepared in good yield from the reactions between $Fe(NO_3)_3 \cdot 9H_2O$ and either Hdppd or Hdmppd in aqueous sodium hydroxide. The products were purified by recrystallisation from dichloromethane-toluene, and the toluene solvate of **1**, $[Fe(dppd)_3] \cdot 1.5C_7H_8$, was characterised crystallographically. The complexes $[Al(dppd)_3]$ **3** and $[Al(dmppd)_3]$ **4** were prepared in an analogous manner using $Al(NO_3)_3 \cdot 9H_2O$. X-ray diffraction showed that **3** crystallised from dichloromethane-toluene as the toluene solvate (**3**$\cdot 1.25C_7H_8$), whereas **4** crystallised from chloroform as **4**$\cdot 4CHCl_3$.

[$Cu(dppd)_2$] **5** was prepared as a DMSO solvate from the reaction between $CuCl_2 \cdot 2H_2O$ and Hdppd in acetonitrile/DMSO in the presence of aqueous sodium hydroxide. [$Zn(dmppd)_2$] **6** was prepared from the metathesis reaction of the aluminium complex **4** with zinc(II) acetate. The reaction between europium(III) chloride and Hdmppd in ethanol in the presence of potassium *tert*-butoxide gave crystals of $[Eu(dmppd)_2(H_2O)_4]Cl \cdot 2EtOH \cdot 0.5H_2O$ **7** while the analogous reaction with lanthanum(III) nitrate gave crystals of $[La(dmppd)_3(H_2O)] \cdot 2H_2O$ **8**.

The structure of $[Fe(dppd)_3] \cdot 1.5C_7H_8$ ($1 \cdot 1.5C_7H_8$)

The compound [$Fe(dppd)_3$] **1** crystallises from dichloromethane-toluene with one molecule of the complex, one full molecule of toluene and a toluene fragment within the asymmetric unit. The iron centre exhibits distorted octahedral geometry, coordinating to three bidentate dppd ligands, as shown in Figure 1a. The Fe–O bond lengths range from 1.9773(11) to 2.0069(11) Å, with ligand bite angles between 85.48(4) and 88.16(4)°. The metal centre lies outside the O_2C_3 mean plane of each ligand, with fold angles, defined as the angles between the FeO_2 and O_2C_3 mean planes, of 18°, 26° and 29° for the three independent ligands. These distortions are considerably larger than those reported by Carlucci and co-workers[17] for the structure of **1** crystallised from THF, which crystallises in a different space group (*Pbcn* as opposed to *P*–1 for $\mathbf{1} \cdot 1.5C_7H_8$) with two complex molecules in the asymmetric unit. The fold angles in the orthorhombic structure are between 5 and 11° for one independent molecule, and 0° and 19° for the other. Overall, the differences between these values and those reported here for $\mathbf{1} \cdot 1.5C_7H_8$ suggest that flexing of the ligand in this manner is a relatively low energy process.

The distortions in **1**·1.5C_7H_8 ensure that the complex is not a regular octahedral metalloligand. Indeed, the N···Fe···N angles range from 63.2° to 114.3° for the '*cis*' pyridyl groups and from 159.3° to 166.5° for the '*trans*' pyridyl groups, while the distances between the nitrogen atoms range from 7.22 Å to 11.64 Å for the '*cis*' pyridyl groups, and from 13.54 Å to 13.79 Å for the '*trans*' pyridyl groups.

The crystal structure of **1**·1.5C_7H_8 contains both enantiomers of **1**. Enantiomeric pairs pack to form dimers *via* C–H···N hydrogen bonds [C(7)···N(3) 3.44 Å, H(7)···N(3) 2.56 Å, C(7)–H(7)···N(3) 154°], as shown in Figure 1b. There is also π···π stacking between some of the dppd ligands. These interactions contribute to the formation of channels in the gross structure which house the included toluene molecules.

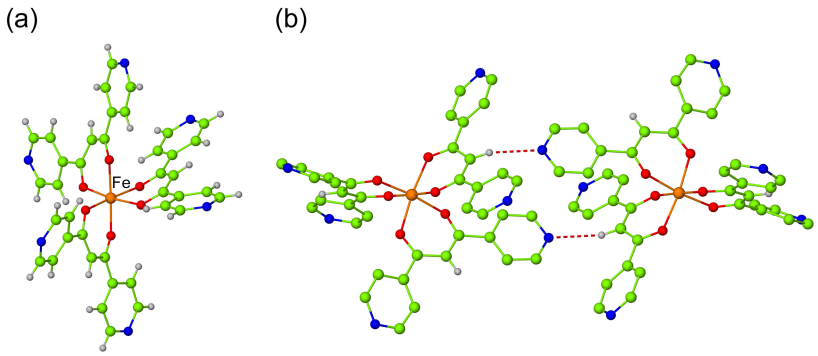

Figure 1. The crystal structure of [Fe(dppd)$_3$]·1.5C_7H_8 (**1**·1.5C_7H_8) showing (a) the [Fe(dppd)$_3$] metalloligand, and (b) C–H···N interactions between molecules of [Fe(dppd)$_3$], linking them into dimers. In (b), the pyridyl hydrogen atoms have been omitted for clarity.

The structures of [Al(dppd)$_3$]·1.25C_7H_8 (3·1.25C_7H_8) and [Al(dmppd)$_3$]·4$CHCl_3$ (4·4$CHCl_3$)

The crystal structure of **3**·1.25C_7H_8 was reported previously[16] and is isostructural to that

of **1**·1.5C_7H_8 so only the key points are summarised here. The complex adopts distorted octahedral geometry around the aluminium centre with Al–O bond lengths ranging between 1.8744(13) and 1.8913(13) Å and ligand bite angles between 88.84(6) and 91.27(6)°. As with **1**·1.5C_7H_8, the chelate rings are non-planar, exhibiting fold angles of 18°, 16° and 26° for the three ligands. The N···N distances between pyridyl nitrogen atoms range from 7.43 to 11.40 Å for the *cis* positions of the octahedron and from 13.39 to 13.59 Å for the *trans* positions. The molecular structure of **3** is shown in Figure 2a.

The asymmetric unit of **4**·4$CHCl_3$ consists of two complex molecules, each containing an aluminium centre and three dmppd ligands, in addition to eight molecules of chloroform. The differences between the two independent molecules of [Al(dmppd)$_3$] are minimal, and one of these is shown in Figure 2b. The aluminium centres display distorted octahedral coordination spheres, with Al–O bond lengths in the range 1.868(4) – 1.894(4) Å. Distortions from a regular octahedral geometry are relatively small, with *trans* bond angles spanning 177.10(19) to 179.62(19)°, and *cis* angles between 87.23(18) and 91.86(18)°.

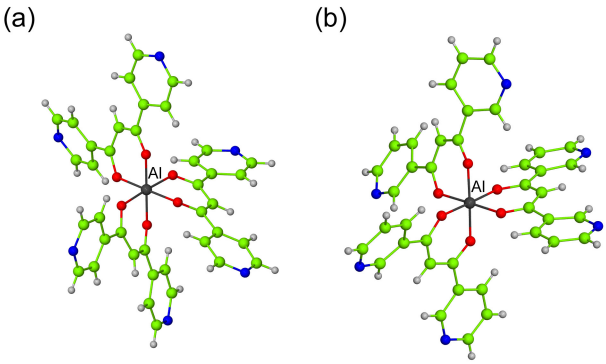

Figure 2. The molecular structures of (a) [Al(dppd)$_3$] **3** in the crystal structure of **3**·1.5C_7H_8, and (b) one of the two independent molecules of [Al(dmppd)$_3$] **4** in the crystal structure of **4**·4$CHCl_3$.

In contrast to dppd, the dmppd ligand can adopt three main conformations depending on the relative positions of the pyridyl nitrogen atoms and the β-diketonate group.

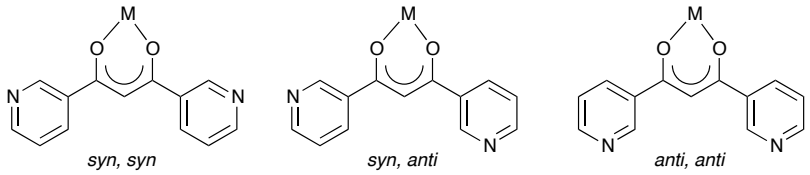

In both of the independent complex molecules of **4**, two of the ligands are in the *anti,anti* conformation, with the nitrogen donors orientated away from the aluminium centre, whereas the third is in the *syn,syn* conformation (Figure 2b).

In each [Al(dmppd)$_3$] molecule, the ligand with *syn,syn* conformation shows the biggest distortions from planarity. This is witnessed by fold angles of 17° and 20° between the O_2Al plane and the mean C_3O_2 plane of the ligand chelate ring (*cf.* values of 2 – 10° for those in the *anti,anti* conformation) and also angles of 48° and 53° between the pyridyl planes in the *syn,syn* ligands (*cf.* values of 8 – 26° for those in the *anti,anti* conformation).

The [Al(dmppd)$_3$] molecules in **4**·4$CHCl_3$ pack into layers, which are separated by the included chloroform molecules. The supramolecular structure of **4**·4$CHCl_3$ contains C–H···N and C–H···O interactions together with π···π interactions between the [Al(dmppd)$_3$] molecules. In addition, there are relatively short C–H···N interactions between the included chloroform molecules and the pyridyl groups.

The structure of [Cu(dppd)$_2$]·DMSO 5

The asymmetric unit of **5** consists of a copper centre, two dppd ligands and an included DMSO molecule. The copper adopts a distorted octahedral coordination geometry, with two dppd ligands coordinated as β-diketonates in the equatorial plane [Cu–O 1.951(2) – 1.966(2) Å] and two pyridyl nitrogen atoms [Cu–N 2.413(3) and 2.415(3) Å] coordinated into the axial positions (Figure 3a). The ligand bite angles are 92.87(10) and 93.47(10)°. The fold angle for each independent ligands is 6°, ensuring that the [Cu(β-diketonate)$_2$] unit is almost flat.

Coordination of half of the pyridyl groups to neighbouring copper(II) centres links the discrete square-planar Cu(dppd)$_2$ molecules into an extended two-dimensional network. Each dppd ligand bridges between two copper centres (one through the β-diketonate, one through a pyridyl ring), leading to the formation of (4,4) sheets (Figure 3b).

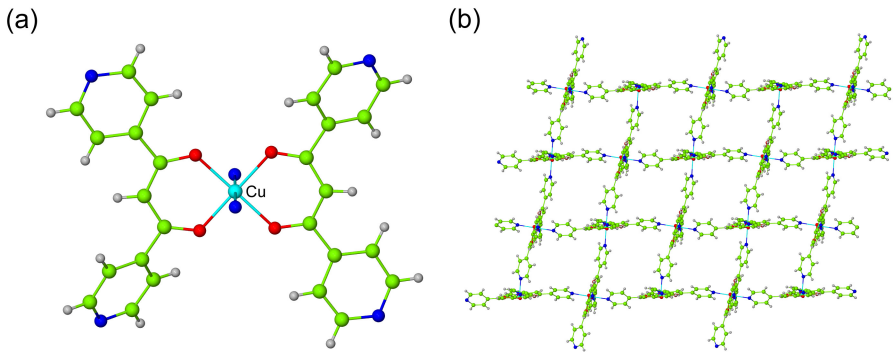

Figure 3. The crystal structure of [Cu(dppd)$_2$]·DMSO **5**, showing (a) one of the [Cu(dppd)$_2$] metalloligands coordinated to two nitrogen atoms from neighbouring metalloligands, and (b) part of the two-dimensional network adopted by **5**.

C–H···O interactions are observed between the pyridyl rings that are not involved in network formation and the included DMSO molecules. However, the uncoordinated nitrogen atoms project into pockets between neighbouring pyridyl rings, and do not form strong intermolecular interactions.

The structure of [Zn(dmppd)$_2$] 6

The asymmetric unit of **6** consists of half of a zinc centre, located on a crystallographic inversion centre, and a dmppd ligand. The remainder of the coordination sphere is generated by symmetry, such that the zinc centre exhibits distorted octahedral geometry, coordinated to two dmppd ligands as *O,O'*-donors in the equatorial plane and to two pyridyl nitrogen atoms in the axial positions (Figure 4a). The Zn–O distances are 2.061(2) and 2.070(2) Å, and the Zn–N distance 2.166(3) Å. The *cis* bond angles around the metal centre lie in the range 86.93(9) – 93.07(9)°, and the ligand bite angle is 89.07(8)°. The dmppd ligands adopt the *syn,anti* conformation, with the *anti* pyridyl groups coordinated to neighbouring zinc centres. The fold angle between the mean ZnO_2 and O_2C_3 planes is 3°.

Coordination of the *anti* pyridyl groups to neighbouring zinc(II) centres connects the Zn(dmppd)$_2$ molecules into a two-dimensional network, as shown in Figure 4b. Each dmppd ligand bridges between two zinc centres (one through the β-diketonate, one through the pyridyl) rendering a network with (4,4) topology, in a similar manner to **5**. The *syn* pyridyl groups are not coordinated, but are involved in C–H···N interactions [C(11)···N(1) 3.369, H(11)···N(1) 2.51 Å, C(11)–H(11)···N(1) 152°]. These interactions link the sheets into a three-dimensional structure.

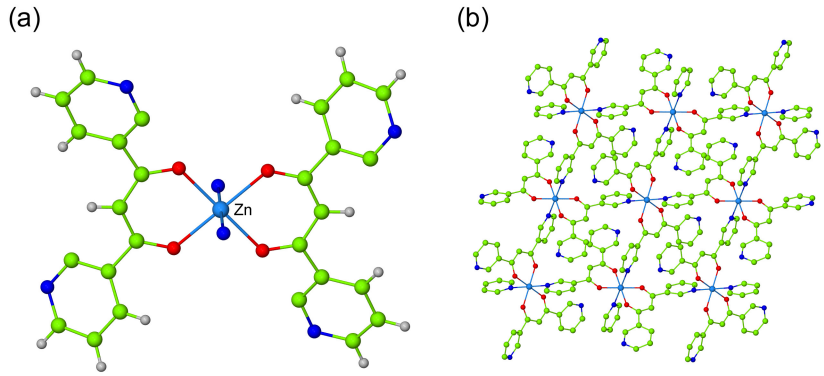

Figure 4. The crystal structure of [Zn(dmppd)$_2$] **6**, showing (a) one of the [Zn(dmppd)$_2$] metalloligands coordinated to two nitrogen atoms from neighbouring metalloligands, and (b) part of the two-dimensional network adopted by **6**, with hydrogen atoms omitted for clarity.

The structure of [Eu(dmppd)$_2$(H$_2$O)$_4$]Cl·2EtOH·0.5H$_2$O 7

The asymmetric unit for **7** consists of one europium atom, two dmppd ligands, four coordinated water molecules, one chloride counter ion disordered over two sites, two ethanol guest molecules disordered over three sites and half of a water molecule.

The europium centre is eight coordinate with approximate square anti-prismatic geometry. The coordination sphere comprises of four Eu–O bonds involving two bidentate dmppd ligands [2.374(5) – 2.396(4) Å] and four Eu–O bonds with coordinated water molecules [2.388(4) – 2.430(4) Å]. Both dmppd ligands adopt the *anti,anti* geometry and have bite angles of 70.18(15)° and 70.38(13)°. The reduced bite angles with respect to the first row *d*-block and aluminium complexes reflects the larger size of europium(III), and the greater Eu–O bond distances. The EuO_2C_3 chelate rings are approximately planar, with angles between the EuO_2 planes and the mean C_3O_2 planes of 1° and 2°. The structure of the [Eu(dmppd)$_2$(H$_2$O)$_4$]$^+$ cation is shown in Figure 5a.

As there is no coordination of the pyridyl nitrogen atoms to neighbouring metal centres, compound **7** contains discrete complex cations. However, the structure is linked into two-dimensional sheets by short O–H···N hydrogen bonds between the coordinated water molecules and the pyridyl groups on neighbouring molecules [O(6)···N(1) 2.750, H(6B)···N(1) 1.85 Å, O(6)–H(6B)···N(1) 173°; O(7)···N(2) 2.742, H(7B)···N(2) 1.85 Å, O(7)–H(7B)···N(2) 171°; O(5)···N(3) 2.714, H(5B)···N(3) 1.86 Å, O(5)–H(5B)···N(3) 159°; O(8)···N(4) 2.760, H(8A)···N(4) 1.87 Å, O(8)–H(8A)···N(4) 169°]. The sheets have a (4,4) topology, though with two linkers between each node (Figure 5b).

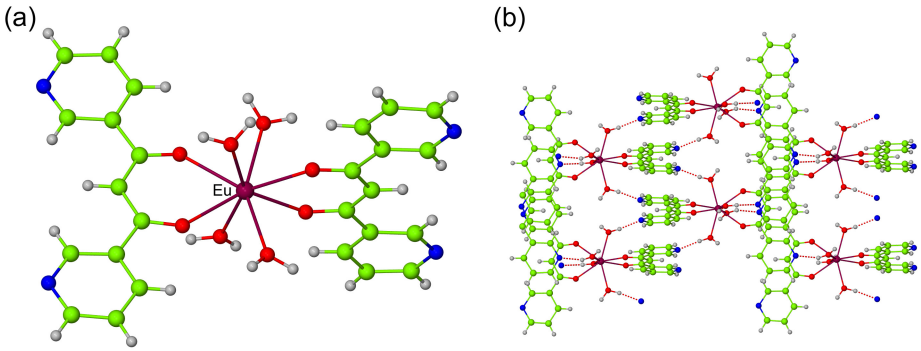

Figure 5. The crystal structure of $[Eu(dmppd)_2(H_2O)_4]Cl{\cdot}2EtOH{\cdot}0.5H_2O$ **7**, showing (a) one of the $[Eu(dmppd)_2(H_2O)_4]^+$ cations, and (b) part of the cationic hydrogen-bonded network adopted by **7**.

The chloride ions lie between the cationic sheets and form hydrogen bonds with the coordinated water ligands. In addition, there are hydrogen bonds between the coordinated water molecules and the included solvent molecules. However, there are no interactions present between neighbouring two dimensional sheets.

The structure of $[La(dmppd)_3(H_2O)]\cdot 2H_2O$ 8

Compound **8** has an asymmetric unit consisting of one lanthanum centre, three coordinated dmppd ligands and one coordinated water molecule. There are also two guest water molecules included within the lattice.

Each lanthanum centre is nine coordinate with distorted tricapped trigonal prismatic geometry. It is coordinated to six oxygen atoms from three dmppd ligands [La(1)–O 2.462(5) – 2.520(5) Å, bite angles 66.64(17) – 68.19(17)°], one oxygen atom from a coordinated water molecule [La(1)–O(7) 2.640(5) Å] and two nitrogen atoms from pyridyl groups on diketonates coordinated to adjacent metal centres [La(1)–N(1) 2.725(6), La(1)–N(6) 2.816(7) Å]. The LaO_2C_3 chelate rings are non-planar, with the lanthanum atom sitting out of plane of the ligand atoms in each of the three rings. The fold angles between the LaO_2 and O_2C_3 mean planes reflect this distortion with values of 8°, 18° and 20° for the three β-diketonates. The three dmppd ligands adopt the *syn,anti* conformation, as shown in Figure 6a.

The coordination of the lanthanum centres to two pyridyl nitrogen atoms from adjacent complexes causes the structure to build up into double-stranded one-dimensional polymeric chains, as depicted in Figure 6b. The pyridyl nitrogen atoms directed to either side of these chains are not coordinated, and as a consequence the framework does not aggregate further through coordination. A two-dimensional network, however, is generated through formation of O–H···N hydrogen bonds, involving the coordinated water ligand and uncoordinated pyridyl groups [O(7)···N(3) 2.946 Å]. Further hydrogen bonds are present between the included water molecules and the uncoordinated pyridyl groups, as well as between the water molecules.

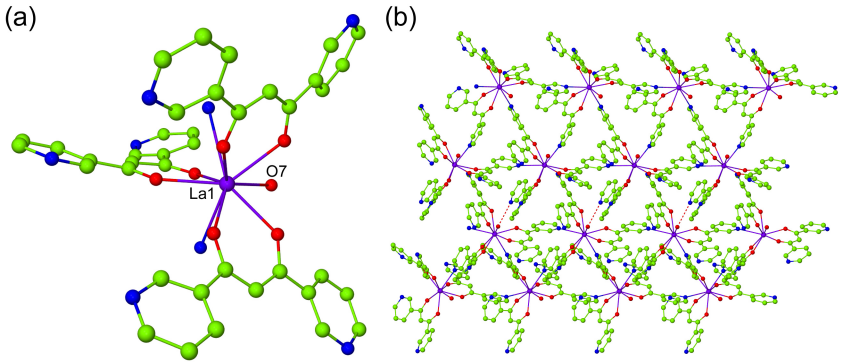

Figure 6. The crystal structure of $[La(dmppd)_3(H_2O)]\cdot 2H_2O$ **8**, showing (a) one of the $[La(dmppd)_3(H_2O)]$ metalloligands, and (b) two double-stranded chains linked together by hydrogen bonding in the structure of **8**. Hydrogen atoms have been omitted for clarity.

The formula of **8** is similar to that of the previously reported compound $[Gd(dppd)_3(H_2O)]\cdot 4H_2O$.[14] In the structure of this gadolinium compound, one of the pyridyl nitrogen atoms coordinates to an adjacent metal centre creating a one-dimensional chain structure. In contrast to this, in **8** two pyridyl nitrogen atoms coordinate to the lanthanum centres leading to the formation of double-stranded one-dimensional chains. This difference is related more to the larger size of the lanthanum(III) centre than the position of the pyridyl groups in dppd and dmppd. Hence, the lanthanum centre in **8** is nine-coordinate, and able to coordinate to two pyridyl groups in addition to three β-diketonates and a water molecule, whereas the smaller gadolinium(III) centre is eight-coordinate, and bonded to only one pyridyl group as well as the three β-diketonates and a water molecule.

Reactions of $[Fe(dppd)_3]$ 1 and $[Fe(dmppd)_3]$ 2 with silver(I) salts

Reactions of the iron metalloligands **1** and **2** with silver(I) salts were carried out in a range of solvents, and those conducted in DMSO or DMSO-acetonitrile afforded crystals

suitable for X-ray analysis for the reactions between **1**·1.5C_7H_8 and silver(I) tetrafluoroborate, silver(I) hexafluorophosphate and silver(I) hexafluoroantimonate. In contrast, reactions involving **2** did not give crystals in these solvents, though crystals were obtained from the reactions between **2** and either silver(I) nitrate or silver(I) trifluoroacetate in dichloromethane-acetonitrile.

The structure of [AgFe(dppd)$_3$]BF_4·2DMSO·2H_2O 9

The asymmetric unit of **9** contains half of an iron centre, coordinated to one and a half dppd ligands, half of a silver centre, half a tetrafluoroborate anion, a DMSO molecule and a water molecule. The iron centre in **9** exhibits distorted octahedral geometry, broadly similar to the geometry of the metalloligand in the structure of **1**·1.5C_7H_8. The Fe–O bond distances have a narrower range than in the parent metalloligand structure [1.988(2) – 1.996(2) Å] as do the bite angles [86.54(12), 86.80(11)°]. Two of the ligands (related by symmetry) have fold angles of 19°, whereas the other is essentially planar (0.3°), meaning the overall distortions from a regular octahedral metalloligand are less than those in **1**·1.5C_7H_8. The silver centre in **9** has a distorted tetrahedral geometry, and is coordinated to four pyridyl nitrogen atoms, with Ag–N bond lengths from 2.256(2) to 2.351(3) Å, and bond angles of between 100.81(15) and 134.39(14)°.

For each Fe(dppd)$_3$ metalloligand, four of the six nitrogen donors are coordinated to silver centres, with one dppd ligand bonded to two silver centres and two symmetry-related ligands bonding each to one silver centre. Given this, the Fe(dppd)$_3$ metalloligand acts as a four-coordinate node with approximate disphenoidal ('saw-horse') geometry (Figure 7a). The coordinated pyridyl groups can be divided into two groups: equatorial, with a N···Fe···N

angle of 91.5°, and axial, with a N···Fe···N angle of 167.8°. The 'equatorial' pyridyl groups are linked through coordination of the silver centres into macrocycles that contain three silver atoms and three Fe(dppd) fragments (Figure 7b). These macrocycles are connected into nanotubes that propagate along the crystallographic *c*-axis. The nanotubes are hexagonally-packed, such that the non-coordinated pyridyl groups interdigitate with those of neighbouring nanotubes in the interstitial space between them (Figure 7c).

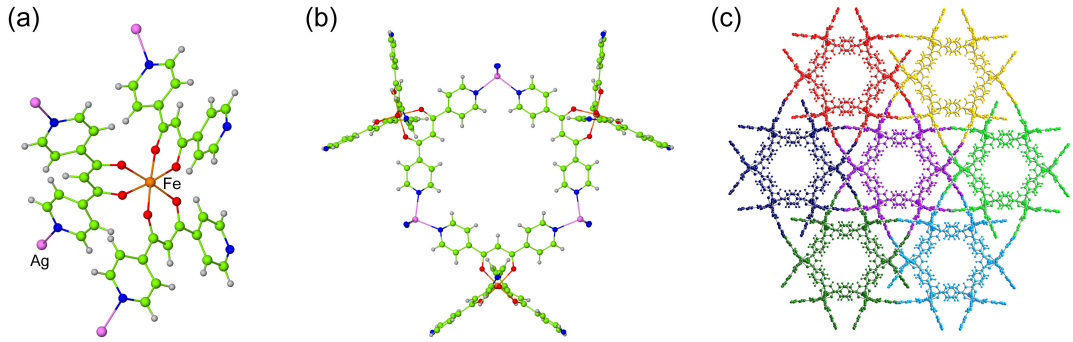

Figure 7. The structure of $[AgFe(dppd)_3]BF_4 \cdot 2DMSO \cdot 2H_2O$ **9**, showing (a) coordination of four silver(I) centres to the $Fe(dppd)_3$ metalloligand, (b) linking of the metalloligands into macrocycles, and (c) the gross structure of **9**, with discrete nanotubes shown in different colours.

Taking into account the van der Waals radii of the atoms, the internal width of the nanotubes, estimated by the shortest edge-of-atom to edge-of-atom distance across the hexagonal pore, is 7.4 Å. The disordered tetrafluoroborate anions are accommodated inside the nanotubes, towards the circumference, reducing the available internal width to approximately 5.3 Å. The included DMSO and water molecules are contained in the interstitial gaps between the nanotubes. Although the hydrogen atoms on the water molecules were not located, the O···O distances (2.791 Å, 2.845 Å) indicate that three water molecules and three DMSO oxygen atoms interact through hydrogen bonds to form 12-membered rings [graph set $R_6^3(12)$].

The structure observed for **9** differs from that reported by Carlucci and co-workers for $[AgFe(dppd)_3]BF_4 \cdot 4THF$ which has a layer structure,[17] despite having a similar metalloligand to **9**, with four of the six pyridyl groups coordinated to silver centres. The structure of $[Ag_5\{Fe(dppd)_3\}_3](tosylate)_5$ contains nanotubes similar to those observed in **9**, though in this instance individual nanotubes are linked together by further silver(I) centres to give a three-dimensional structure.[17]

The structure of $[AgFe(dppd)_3]PF_6 \cdot 3.28DMSO$ 10

The asymmetric unit of **10** consists of half of an iron atom coordinated to one and a half dppd ligands, half of a silver atom, half of a hexafluorophosphate anion, and two DMSO molecules with fractional occupation. The iron, silver and phosphorus atoms are all located at crystallographic special positions.

The coordination sphere about the iron centre in **10** has distorted octahedral geometry, broadly similar to the geometry of the metalloligand $Fe(dppd)_3$ in $\mathbf{1} \cdot 1.5C_7H_8$ and to that in **9**. The Fe–O bond distances lie in the range 1.991(6) – 2.367(8) Å, with bite angles of 86.5(2) and 87.0(2)°. Two of the ligands (related by symmetry) have fold angles of 16°, whereas the other is much closer to planarity (2°). The silver centre displays a distorted tetrahedral geometry, and is coordinated to four pyridyl nitrogen atoms, with Ag–N bond lengths ranging from 2.255(6) to 2.367(8) Å, and N–Ag–N bond angles of between 95.1(3) and 135.5(4)°.

As with **9**, each $Fe(dppd)_3$ metalloligand in **10** has four of the six nitrogen donors coordinated to silver centres, with one dppd ligand bonded to two silver centres and the two symmetry-related ligands each bonding to one silver centre, with the resultant four-coordinate node

having a similar geometry to that in **9** (Figure 8a). Despite the similarities in the building blocks in **9** and **10**, the gross structures are very different. In **10**, coordination of the 'equatorial' nitrogen atoms to silver centres connects the metalloligands into chains. These are cross-linked by coordination of the 'axial' nitrogen atoms to silver centres into corrugated two-dimensional layers with (4,4) topology (**sql**)[18] (Figure 8b,c).

There are two types of diamond-shaped pores in the network adopted by **10**. Half are capped by uncoordinated pyridyl groups, and these accommodate some of the included DMSO solvent molecules. The other half are open and contain the hexafluorophosphate anions. The remaining DMSO is included between the layers. There is evidence for the presence of C–H···N interactions between the methyl groups of the DMSO molecules and the uncoordinated pyridyl groups. The network structure observed for **10** is similar to that reported recently for the THF solvate.[17]

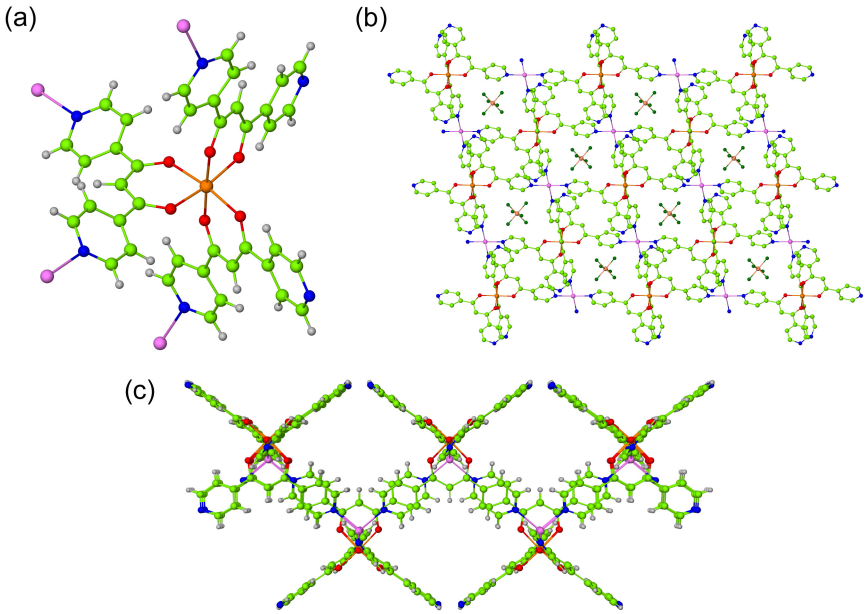

Figure 8. The structure of $[AgFe(dppd)_3]PF_6 \cdot 3.28DMSO$ **10**, showing (a) coordination of four silver(I) centres to the $Fe(dppd)_3$ metalloligand, (b) linking of the metalloligands into

layers showing the positions occupied by the hexafluorophosphate anions, with hydrogen atoms omitted for clarity, and (c) a side-on view of one of the layers.

The structure of $[AgFe(dppd)_3]SbF_6 \cdot 1.25DMSO$ 11

The asymmetric unit of **11** consists of one iron atom coordinated to three crystallographically independent dppd ligands, one silver atom, one hexafluoroantimonate anion, and a disordered DMSO molecule. An additional highly disordered fragment of DMSO was also present, and estimated as a quarter molecule per asymmetric unit.

The iron centre in **11** exhibits distorted octahedral geometry, broadly similar to the geometry in the metalloligand $Fe(dppd)_3$ in the structure of $\mathbf{1} \cdot 1.5C_7H_8$ and to those in **9** and **10**. The Fe–O bond distances lie in the narrow range 1.981(4) – 1.992(2) Å, with bite angles of 85.56(16), 86.89(16) and 86.94(15)°. For all of the ligands, the iron centre lies outside the O_2C_3 plane, with fold angles of 13°, 18° and 27°. The silver centre is distorted tetrahedral in geometry, coordinated to four nitrogen atoms, with Ag–N bond lengths between 2.245(5) and 2.381(5) Å, and bond angles of between 91.24(18) and 144.69(18)°, indicating larger distortions from the ideal geometry than observed in **9** and **10**.

In a similar manner to that observed in **9** and **10**, each $Fe(dppd)_3$ moeity in **11** has four of the six available nitrogen donors coordinated to silver centres. One dppd ligand is bonded to two silver centres while the other two dppd ligands are each bonded to one silver centre. The resultant four-coordinate node has a similar geometry to those in **9** and **10** (Figure 9a). As with **10**, the silver centres link the iron metalloligands into two-dimensional layers with (4,4) topology (Figure 9b). Although the layers have the same topology as those in **10**, there are

differences in the degree of corrugation, with the layers in **11** considerably more undulated than those in **10** (Figure 9c).

In the gross structure of **11**, the disordered hexafluoroantimonate anions are proximate to some of the diamond-shaped pores. One of the uncoordinated pyridyl groups is involved in C–H···N interactions with aryl groups from a neighbouring layer [C(10)···N(5) 3.482 Å, H(10)···N(5) 2.54 Å, C(10)–H(10)···N(5) 170°]. Carlucci and co-workers recently reported that the THF solvate $[AgFe(dppd)_3]SbF_6 \cdot 4THF$ is isostructural with the hexafluorophosphate analogue[17] (and, by extension, with **9**). Hence, with hexafluoroantimonate-containing iron-silver network structures, a change in the solvate leads to subtle changes in the manner in which the sheets pack.

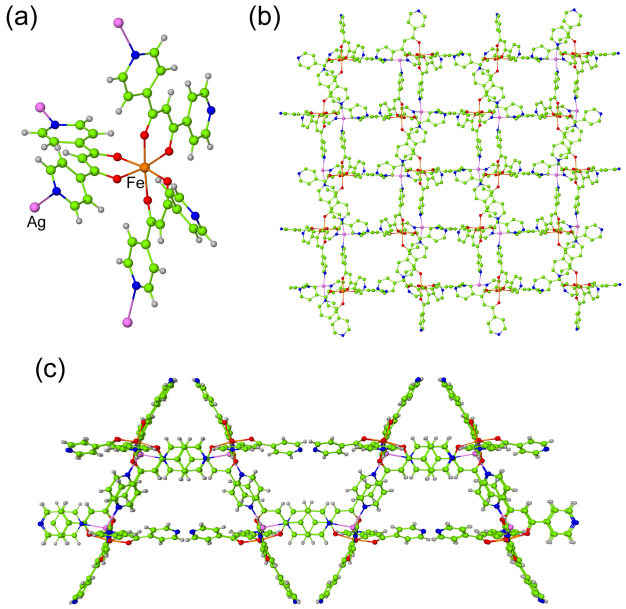

Figure 9. The structure of $[AgFe(dppd)_3]SbF_6 \cdot 1.25DMSO$ **11**, showing (a) coordination of four silver(I) centres to the $Fe(dppd)_3$ metalloligand, (b) linking of the metalloligands into layers, with hydrogen atoms omitted for clarity, and (c) a side-on view of one of the layers.

The structure of $[Ag_2Fe(dmppd)_3(ONO_2)]NO_3 \cdot MeCN \cdot CH_2Cl_2$ 12

The asymmetric unit of **12** consists of one iron atom coordinated to three crystallographically independent dmppd ligands, two silver atoms, two nitrate anions, an acetonitrile molecule and a dichloromethane molecule. The iron centre demonstrates distorted octahedral geometry, maintaining the structure of the metalloligand. The Fe–O distances range from 1.966(5) to 1.996(5) Å, with ligand bite angles of 85.50(18), 85.77(19) and 86.50(19)°. All of the pyridyl nitrogen atoms are coordinated to silver centres.

One of the ligands in **12** adopts the *syn,syn* conformation whereas the other two adopt the *syn,anti* conformation. For all of the dmppd ligands, the iron centre lies outside the O_2C_3 plane, with greater fold angles for the *syn,anti*-ligands (24°, 26°) than for the *syn,syn*-ligand (10°). The geometry about the silver centres is distorted tetrahedral by virtue of coordination to three nitrogen atoms and one oxygen atom, the latter from a nitrate ion. The Ag–N bond lengths range from 2.237(5) to 2.356(6) Å, with Ag–O bond lengths of 2.483(6) and 2.528(6) Å. Bond angles lie between 83.8(2) and 119.7(2)° for Ag(1) and between 87.2(2) and 120.1(2)° for Ag(2). The coordinated oxygen atom bridges between two silver atoms [Ag(1)–O(7)–Ag(2) 152.0(3)°], and since the other nitrate oxygen atoms are uncoordinated, the silver centres can be considered as forming $Ag_2(\mu\text{-}ONO_2)$ hexatopic nodes. Two pairs of nitrogen donors from the *syn,anti*- ligands of each $Fe(dmppd)_3$ metalloligand coordinate to a $Ag_2(\mu\text{-}ONO_2)$ unit (Figure 10a). This links the metalloligands into chains, as shown in Figure 10b. Coordination to the silver centre brings pairs of pyridyl rings close together within the $Fe(dmppd)_3$ metalloligand, and is the source of the distortions evidenced by the large fold angles observed. The chains are cross-linked via coordination of the pyridyl

groups from the *syn,syn*- ligands to the silver centres, leading to the formation of layers (Figure 10c).

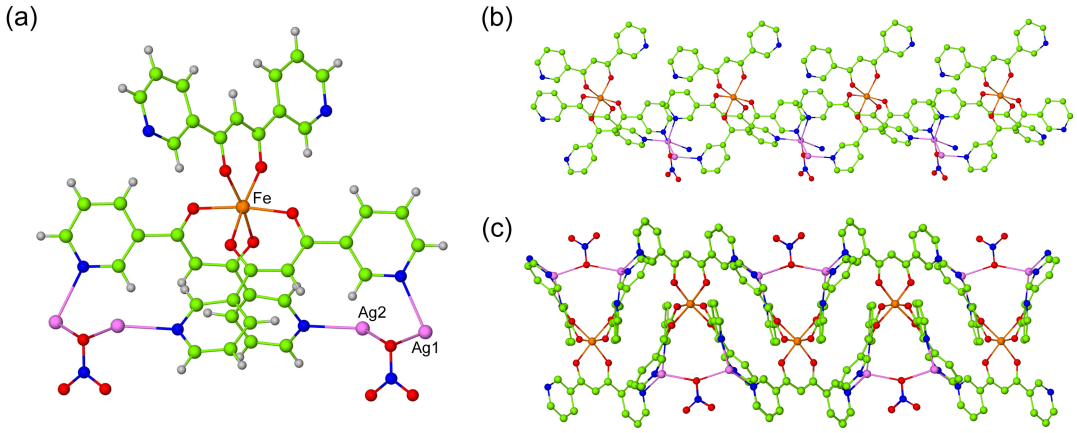

Figure 10. The structure of $[Ag_2Fe(dmppd)_3(ONO_2)]NO_3 \cdot MeCN \cdot CH_2Cl_2$ **12**, showing (a) coordination of six silver(I) centres to the $Fe(dmppd)_3$ metalloligand and the bridging nitrate groups, (b) linking of the metalloligands into chains, and (c) a side-on view of one of the layers. In (b) and (c) hydrogen atoms have been omitted for clarity.

By regarding each $Ag_2(\mu\text{-}ONO_2)$ unit and $Fe(dmppd)_3$ metalloligand as nodes, the resultant network is of (4,4) topology (**sql**), since each $Ag_2(\mu\text{-}ONO_2)$ unit coordinates to four different iron centres, while each $Fe(dmppd)_3$ metalloligand coordinates to four different $Ag_2(\mu\text{-}ONO_2)$ units. Omitting the nitrate from the analysis changes the network to **kgd** topology, with the $Fe(dmppd)_3$ metalloligand coordinated to six silver centres, and each silver coordinated to three metalloligands.

The included solvent and uncoordinated nitrate ions lie between the layers. The dichloromethane molecules form C–H···O interactions with the uncoordinated oxygen atoms of the nitrate ligand [C(42)···O(9) 3.305, H(42A)···O(9) 2.48 Å, C(42)–H(42A)···O(9) 140°; C(42)···O(8) 3.359, H(42B)···O(8) 2.46 Å, C(42)–H(42B)···O(8) 151°], leading to the

formation of $R_4^4(12)$ graph sets. The uncoordinated nitrate ion also forms C–H···O interactions, with an aryl hydrogen atom acting as the donor [C(39)···O(10) 3.384, H(39)···O(10) 2.44 Å, C(39)–H(39)···O(10) 172°].

The structure of $[Ag_2Fe(dmppd)_3(O_2CCF_3)]CF_3CO_2 \cdot 2MeCN \cdot 0.25CH_2Cl_2$ 13

The asymmetric unit of **13** consists of one iron atom coordinated to three crystallographically independent dmppd ligands, two silver atoms, two trifluoroacetate anions, two acetonitrile molecules and a fractional portion of a dichloromethane molecule. The iron centre has distorted octahedral geometry, and the Fe–O distances range from 1.975(4) to 2.022(4) Å, with ligand bite angles of 85.46(16), 85.53(15) and 87.39(16)°. The silver(I) centres exhibit distorted tetrahedral geometry, with each coordinated to three nitrogen atoms (Ag–N 2.254(5) – 2.370(5) Å) and one oxygen atom (Ag–O 2.426(4), 2.441(5) Å). Bond angles at the silver centres range between 84.30(16) and 134.44(18)° for Ag(1) and between 99.67(16) and 124.76(19)° for Ag(2).

The building blocks present in the structure of **13** are very similar to those in **12**. Thus, for the metalloligands, one dmppd ligand is in the *syn,syn* conformation and the other two are in the *syn,anti* conformation, and the largest distortions are in the *syn,anti* ligands as witnessed by fold angles of 30° and 32° (compare 13° for the *syn,syn* ligand). All six pyridyl nitrogen atoms are coordinated in the gross structure. One of the trifluoroacetate ions bridges between the two independent silver centres through one oxygen atom to give $Ag_2(\mu\text{-}O_2CCF_3)$ units, with an Ag–O–Ag angle of 109.63(17)°. The resultant network is similar to that observed for **12**, with the $Ag_2(\mu\text{-}O_2CCF_3)$ units in **13** playing a similar structural role to the $Ag_2(\mu\text{-}ONO_2)$ units in **12**. There are differences between the supramolecular interactions observed in **12**

and **13**. Thus, in **13**, C–H···O interactions are observed between the coordinated trifluoroacetate and an aryl hydrogen atom as opposed to a dichloromethane molecule [C(7)···O(8) 3.241, H(7)···O(8) 2.30 Å, C(7)–H(7)···O(8) 171°].

Discussion

The crystal structures reported in this paper, together with that of $[Eu(Hdppd)_3(H_2dppd)]Cl_4 \cdot EtOH$ reported earlier,[16] reveal it is possible to coordinate between two and four dppd or dmppd ligands to a metal centre, depending on the size and coordination preference of the metal centre, though the reaction conditions also have a significant effect on the product isolated from the reaction. Although, at first sight, the ligands might appear to be relatively rigid, there is considerable flexibility in their conformations, evidenced largely by the wide range of fold angles observed as a consequence of bending about the ligand O···O vector. Thus the angle between MO_2 and O_2C_3 mean planes has been shown to vary from 0° to 32°.

Compounds **4**, **6**–**8**, **12** and **13** contain dmppd ligands. Of the 18 crystallographically independent dmppd ligands in these six structures, six adopt the *anti,anti* conformation, eight adopt the *syn,anti* conformation and four adopt the *syn,syn* conformation. In the single-metal systems, coordination (in **6**, **8**) or strong hydrogen bond formation (in **7**, **8**) is observed only for the *anti*-pyridyl groups, though in the iron-silver compounds (**12**, **13**) both *syn*- and *anti*-pyridyls are coordinated.

In contrast to the reaction of either $[Al(dppd)_3]$ or $[Ga(dppd)_3]$ with silver nitrate, reaction of $[Fe(dppd)_3] \cdot 1.5C_7H_8$ with a range of silver salts does not give a structure in which all of the

pyridyl groups are bridged by silver centres into a cubic network. Indeed, in the structures of **9-11** only four of the six pyridyl groups are coordinated. In these compounds, one ligand coordinates to two silver(I) centres, whereas the other two each coordinate to only one silver(I) centre. This means that the metalloligand building block is similar for **9-11** (see Figures 8a, 9a and 10a), though the architectures of the resultant structures are very different. Figure 11 illustrates schematically how the $Fe(dppd)_3$ and Ag^+ building blocks can combine to give these different architectures, focussing on the dppd ligand that coordinates to two silver centres (*i.e.* the 'equatorial' nitrogen atoms from the disphenoidal metalloligand). In **9**, the angles within the dppd ligands are orientated in the same direction as those around the silver centres, ensuring the formation of macrocycles, which are further linked by coordination of the 'axial' nitrogen atoms into nanotubes. In **10**, the angles within the dppd ligands are orientated in the opposite direction as those around the silver centres, ensuring corrugated sheet formation. Finally, in **11**, the angles in both the dppd ligands and silver centres alternate, leading to formation of a more undulated sheet structure.

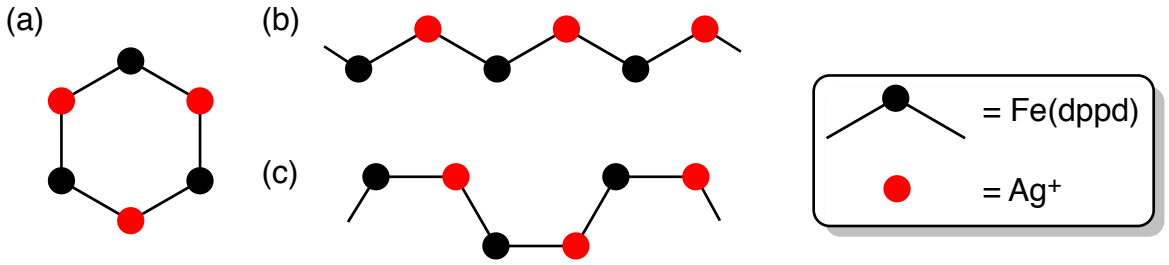

Figure 11. A schematic representation of how Fe(dppd) fragments from $Fe(dppd)_3$ metalloligands and Ag^+ centres can assemble into (a) macrocycles, (b) corrugated chains, and (c) undulating chains. These are further linked into nanotubes (for a) or layers (for b and c).

The structure of **9** is, to the best of our knowledge, the first example of a discrete mixed-metal nanotube structure. Coordination nanotubes have been reported previously,[19] though in many cases terminating ligands have been deliberately included to block further extension of

the network. The structure of $[In(1,3\text{-bdc})_2]^-$ offers the closest parallels to **9**, with indium(III) centres and 1,3-benzenedicarboxylate ligands playing the same structural roles as the silver centres and Fe(dppd) fragments, respectively, in **9**.[20] As noted above, $[Ag_5\{Fe(dppd)_3\}_3](tosylate)_5$ contains similar nanotubes to those in **9**, though in this case individual nanotubes are linked together by further silver(I) centres to gives a three-dimensional gross structure.[17]

Although $[Fe(dppd)_3]$ is very similar in geometry to $[Al(dppd)_3]$, the products from the reactions of the two metalloligands with silver salts are very different. Compounds **9-11** contain a 1:1 ratio of the two metals, whereas $[Ag_3Al(dppd)_3](NO_3)_3 \cdot 4DMSO$ contains a 1:3 ratio. Alteration of the starting material ratios does not affect the product distribution in these reactions, so the ratio of metal centres present in these structures does not have its origins in simple reaction stoichiometry. Although the different counter-ions preclude a direct comparison, it is notable that the iron-silver networks **9-11** crystallise faster than the aluminium-silver network. Hence, one possible explanation is that **9-11** are kinetic rather than thermodynamic products, and the greater solubility of the aluminium complex may be a factor in the observation of more coordinatively saturated products with this *p*-block metalloligand.

Despite all of the pyridyl groups being coordinated in **12** and **13** as they are in $[Ag_3Al(dppd)_3](NO_3)_3 \cdot 4DMSO$, compounds **12** and **13** do not adopt analogous cubic networks. With the pyridyl nitrogen atoms in the 3-positions, the hexatopic metalloligand is far from the octahedral geometry required to give rise to a cubic network, and the relative proximity of some of the pyridyl nitrogen donors enable two of them to coordinate to the same $Ag_2(\mu\text{-}ONO_2)$ or $Ag_2(\mu\text{-}O_2CCF_3)$ fragment. Such motifs are not possible in networks

containing $M(dppd)_3$ metalloligands because of the longer distances between pyridyl nitrogens and the different relative orientations of these donor atoms.

In conclusion, we have shown that dppd and dmppd form complexes with a range of *d*-, *f*- and *p*-block metal centres. Furthermore, the iron(III) complexes $[Fe(dppd)_3]$ and $[Fe(dmppd)_3]$ can act as metalloligands, and the architectures of the networks formed on reaction with silver(I) salts differ from those observed with $[Al(dppd)_3]$. In the three crystallographically characterised mixed-metal networks containing the $Fe(dppd)_3$ metalloligand reported here, the iron complex was observed to act as a disphenoidal tetratopic ligand with two uncoordinated nitrogen atoms as opposed to an octahedral hexatopic ligand. Combination of this metalloligand with tetrahedral silver centres affords a range of different networks, with the structure of **9** being the most noteworthy, as it contains the first example of discrete mixed-metal coordination nanotubes. Comparison between the structures of **9-11** and those recently reported by Carlucci and co-workers[17] demonstrates that the solvent has an important impact on the structure adopted, with both the tetrafluoroborate and hexafluoroantimonate compounds obtained from DMSO adopting different networks to those observed from THF solutions. Current research involves exploring the use of metalloligands based on dppd and dmppd with other metals with the aim of forming more robust networks, and investigations of the properties of **9**.

Experimental

Synthetic details are provided in the ESI. Information about the crystal data collections, solutions and refinements are given in Table 1. Additional information about the crystal structures is provided in the ESI.

Supplementary information

Synthetic and crystallographic details.

Acknowledgements

The EPSRC, the Leverhulme Trust and the Cambridge Crystallographic Data Centre are thanked for financial support. The EPSRC is also thanked for support of the National Mass Spectrometry Service Centre.

References

1. S. Kitagawa, R. Kitaura and S. Noro, *Angew. Chem. Int. Ed.*, 2004, **43**, 2334; G. Férey, *Chem. Soc. Rev.*, 2008, **37**, 191; D. J. Tranchemontagne, J. Mendoza-Cortés, M. O'Keeffe and O. M. Yaghi, *Chem. Soc. Rev.*, 2009, **38**, 1257.
2. S. Kitagawa, S. Noro and T. Nakamura, *Chem. Commun.*, 2006, 701; S. J. Garibay, J. R. Stork and S. M. Cohen, *Prog. Inorg. Chem.*, 2009, **56**, 335.
3. S. Noro, H. Miyasaka, S. Kitagawa, T. Wada, T. Okubo, M. Yamashita and T. Mitani, *Inorg. Chem.*, 2005, **44**, 133; S. M. Humphrey, T. J. P. Angliss, M. Aransay, D. Cave, L. A. Gerrard, G. F. Weldon and P. T. Wood, *Z. Anorg. Allg. Chem.*, 2007, **633**, 2342; A. D. Burrows, M. F. Mahon and C. Wong, *CrystEngComm*, 2008, **10**, 487.
4. R. Kitaura, G. Onoyama, H. Sakamoto, R. Matsuda, S. Noro and S. Kitagawa, *Angew. Chem. Int. Ed.*, 2004, **43**, 2684.
5. O. Guillou, C. Daiguebonne, M. Camara and N. Kerbellec, *Inorg. Chem.*, 2006, **45**, 8468.
6. B. F. Abrahams, B. F. Hoskins, D. M. Michail and R. Robson, *Nature*, 1994, **369**, 727.
7. S. R. Halper, L. Do, J. R. Stork and S. M. Cohen, *J. Am. Chem. Soc.*, 2006, **128**, 15255; J. R. Stork, V. S. Thoi and S. M. Cohen, *Inorg. Chem.*, 2007, **46**, 11213; D. Pogozhev, S. A. Baudron and M. W. Hosseini, *Inorg. Chem.*, 2010, **49**, 331.
8. J. E. Beves, E. C. Constable, C. E. Housecroft, C. J. Kepert and D. J. Price, *CrystEngComm*, 2007, **9**, 456; C. M. Ollagnier, D. Nolan, C. M. Fitchett and S. M. Draper, *Inorg. Chem. Commun.*, 2007, **10**, 1045.
9. K.-T. Youm, M. G. Kim, J. Ko and M.-J. Jun, *Angew. Chem. Int. Ed.*, 2006, **45**, 4003.
10. A. D. Burrows, K. Cassar, M. F. Mahon and J. E. Warren, *Dalton Trans.*, 2007, 2499.
11. L. Carlucci, G. Ciani, S. Maggini, D. M. Proserpio and M. Visconti, *Chem. Eur. J.*, 2010, **16**, 12328.

12. V. D. Vreshch, A. N. Chernega, J. A. K. Howard, J. Sieler and K. V. Domasevitch, *Dalton Trans.*, 2003, 1707; V. D. Vreshch, A. B. Lysenko, A. N. Chernega, J. A. K. Howard, H. Krautscheid, J. Sieler and K. V. Domasevitch, *Dalton Trans.*, 2004, 2899; V. D. Vreshch, A. B. Lysenko, A. N. Chernega, J. Sieler and K. V. Domasevitch, *Polyhedron*, 2005, 10.

13. B. Chen, F. R. Fronczek and A. W. Maverick, *Inorg. Chem.*, 2004, **43**, 8209; Y. Zhang, B. Chen, F. R. Fronczek and A. W. Maverick, *Inorg. Chem.*, 2008, **47**, 4433.

14. P. C. Andrews, G. B. Deacon, R. Frank, B. H. Fraser, P. C. Junk, J. G. MacLellan, M. Massi, B. Moubaraki, K. S. Murray and M. Silberstein, *Eur. J. Inorg. Chem.*, 2009, **2009**, 744.

15. M. Dudek, J. K. Clegg, C. R. K. Glasson, N. Kelly, K. Gloe, K. Gloe, A. Kelling, H. J. Buschmann, K. A. Jolliffe, L. F. Lindoy and G. V. Meehan, *Cryst. Growth Des.*, 2011, **11**, 1697.

16. A. D. Burrows, C. G. Frost, M. F. Mahon, P. R. Raithby, C. L. Renouf, C. Richardson and A. J. Stevenson, *Chem. Commun.*, 2010, **46**, 5067.

17. L. Carlucci, G. Ciani, D. M. Proserpio and M. Visconti, *CrystEngComm*, 2011, **13**, 5891.

18. M. O'Keeffe, M. A. Peskov, S. J. Ramsden and O .M. Yaghi, *Acc. Chem. Res.*, 2008, **41**, 1782.

19. M. Aoyagi, S. Tashiro, M. Tominaga, K. Biradha and M. Fujita, *Chem. Commun.*, 2002, 2036; X.-L. Wang, C. Qin, E.-B. Wang, Y.-G. Li, Z.-M. Su, L. Xu and L. Carlucci, *Angew. Chem. Int. Ed.*, 2005, **44**, 5824; F. Dai, H. He and D. Sun, *J. Am. Chem. Soc.*, 2008, **130**, 14064; X.-C. Huang, W. Luo, Y.-F. Shen, X.-J. Lin and D. Li, *Chem. Commun.*, 2008, 3995; K.-L. Huang, X. Liu, X. Chen and D.-Q. Wang, *Cryst. Growth Des.*, 2009, **9**, 1646; W.-T. Liu, Y.-C. Ou, Y.-L. Xie, Z. Lin and M.-L. Tong, *Eur. J. Inorg. Chem.*, 2009, **2009**, 4213; T.-T. Luo, H.-C. Wu, Y.-C. Jao, S.-M. Huang, T.-W. Tseng, Y.-S. Wen, G.-H. Lee, S.-M. Peng and K.-L. Lu, *Angew. Chem. Int. Ed.*, 2009, **48**, 9461; K. Otsubo, Y. Wakabayashi, J. Ohara, S. Yamamoto, H. Matsuzaki, H. Okamoto, K. Nitta, T. Uruga and H. Kitagawa, *Nature Mater.*, 2011, **10**, 291.

20. F. Bu and S.-J. Xiao, *CrystEngComm*, 2010, **12**, 3385.

Table 1. Crystallographic details for compounds **1**·1.5C_7H_8, **4**·4$CHCl_3$ and **5-13**

Compound reference	**1**·1.5C_7H_8	**4**·4$CHCl_3$	**5**	**6**	**7**	**8**
Chemical formula	$C_{49\cdot5}H_{39}FeN_6O_6$	$C_{43}H_{31}AlCl_{12}N_6O_6$	$C_{28}H_{24}CuN_4O_5S$	$C_{13}H_7N_2O_2Zn_{0\cdot5}$	$C_{30}H_{39}ClEuN_4O_{10\cdot5}$	$C_{39}H_{33}LaN_6O_9$
Formula Mass	869.72	1180.12	592.11	255.89	811.06	868.62
Crystal system	Triclinic	Triclinic	Monoclinic	Monoclinic	Triclinic	Orthorhombic
Space group	$P\bar{1}$	$P\bar{1}$	$P2_1/a$	$P2_1/n$	$P\bar{1}$	$P2_1ca$
a/Å	12.0670(2)	10.2070(2)	14.5630(4)	9.0820(16)	9.8170(3)	9.7470(2)
b/Å	12.6310(2)	15.0570(2)	11.4730(3)	9.9551(17)	12.8910(4)	12.7120(2)
c/Å	14.3780(3)	33.3180(5)	16.3770(6)	13.093(2)	13.8310(6)	31.1260(5)
α/°	87.509(1)	92.341(1)	90.00	90.00	87.802(1)	90.00
β/°	82.407(1)	90.772(1)	100.2890(10)	109.136(3)	79.328(1)	90.00
γ/°	79.667(1)	96.535(1)	90.00	90.00	79.802(2)	90.00
Unit cell volume/Å^3	2136.59(7)	5082.17(14)	2692.29(14)	1118.4(3)	1692.85(10)	3856.63(12)
Temperature/K	150(2)	150(2)	150(2)	150(2)	150(2)	150(2)
No. of formula units per unit cell, Z	2	4	4	4	2	4
Absorption coefficient, μ/mm^{-1}	0.412	0.723	0.935	1.140	1.993	1.170
No. of reflections measured	36317	52542	51590	7824	7615	34837
No. of independent reflections	12398	16879	6155	2259	5673	6696
R_{int}	0.0413	0.0810	0.0922	0.0505	0.0349	0.1384
Final R_1 values ($I > 2\sigma(I)$)	0.0448	0.0962	0.0592	0.0453	0.0477	0.0485
Final $wR(F^2)$ values ($I > 2\sigma(I)$)	0.1096	0.2327	0.1487	0.1116	0.1159	0.0848
Final R_1 values (all data)	0.0758	0.1322	0.1238	0.0598	0.0602	0.0962
Final $wR(F^2)$ values (all data)	0.1214	0.2540	0.1697	0.1208	0.1220	0.0998
Goodness of fit on F^2	1.033	1.050	0.998	1.045	1.124	1.035
Flack parameter						–0.04(2)

Compound reference	**9**	**10**	**11**	**12**	**13**
Chemical formula	$C_{43}H_{43}AgBF_4FeN_6O_{10}S_2$	$C_{45\cdot56}H_{56\cdot28}AgF_6FeN_6O_{9\cdot28}PS_{3\cdot28}$	$C_{41\cdot5}H_{35\cdot5}AgF_6FeN_6O_{7\cdot25}S_{1\cdot25}Sb$	$C_{42}H_{32}Ag_2Cl_2FeN_9O_{12}$	$C_{46\cdot75}H_{32}Ag_2Cl_{0\cdot5}F_6FeN_8O_{10}$
Formula Mass	1118.48	1250.29	1173.80	1197.26	1269.12
Crystal system	Trigonal	Monoclinic	Monoclinic	Triclinic	Triclinic
Space group	$P\bar{3}\,c1$	$C2/c$	$P2_1/c$	$P\bar{1}$	$P\bar{1}$
a/Å	23.5252(4)	13.378(2)	12.0850(1)	11.7140(3)	11.789(2)
b/Å	23.5252(4)	23.544(3)	24.2820(2)	14.0930(5)	13.259(3)
c/Å	17.8727(7)	18.052(3)	18.1190(2)	15.5890(6)	16.790(3)
α/°	90.00	90.00	90.00	100.969(2)	102.365(2)
β/°	90.00	102.387(2)	94.126(1)	109.712(2)	91.136(2)
γ/°	120.00	90.00	90.00	103.542(2)	104.490(2)
Unit cell volume/Å^3	8566.2(4)	5553.3(14)	5303.20(9)	2251.11(13)	2474.6(8)
Temperature/K	150(2)	150(2)	150(2)	150(2)	150(2)
No. of formula units per unit cell, Z	6	4	4	2	2
Absorption coefficient, μ/mm^{-1}	0.735	0.842	1.259	1.371	1.188
No. of reflections measured	69715	8516	96145	32276	17689
No. of independent reflections	8830	2722	12131	32276	17694
R_{int}	0.0731	0.0441	0.0725	0.0000	0.0000
Final R_1 values ($I > 2\sigma(I)$)	0.0495	0.0619	0.0873	0.1066	0.0671
Final $wR(F^2)$ values ($I > 2\sigma(I)$)	0.1452	0.1531	0.2414	0.2402	0.1682
Final R_1 values (all data)	0.0569	0.0768	0.1035	0.1329	0.1045
Final $wR(F^2)$ values (all data)	0.1502	0.1591	0.2544	0.2594	0.1827
Goodness of fit on F^2	1.067	1.110	1.038	1.116	1.047